



HAL
open science

Optical interferometric study on deformation and fracture based on physical mesomechanics

Sanichiro Yoshida

► **To cite this version:**

Sanichiro Yoshida. Optical interferometric study on deformation and fracture based on physical mesomechanics. *Physical Mesomechanics*, 1999, 2 (4), pp.5-12. hal-01092691

HAL Id: hal-01092691

<https://hal.science/hal-01092691>

Submitted on 9 Dec 2014

HAL is a multi-disciplinary open access archive for the deposit and dissemination of scientific research documents, whether they are published or not. The documents may come from teaching and research institutions in France or abroad, or from public or private research centers.

L'archive ouverte pluridisciplinaire **HAL**, est destinée au dépôt et à la diffusion de documents scientifiques de niveau recherche, publiés ou non, émanant des établissements d'enseignement et de recherche français ou étrangers, des laboratoires publics ou privés.

Optical interferometric study on deformation and fracture based on physical mesomechanics

Sanichiro Yoshida

Physics Department, University of Florida, Gainesville, Florida 32611, USA
E-mail: yoshida@phys.ufl.edu

Abstract

This paper discusses an optical band pattern that we recently discovered in an optical interferometric tensile analysis. The most important feature of this band pattern is that it indicates whether the sample is close to failure and where the failure will occur. Previous investigations indicate that this band pattern represents stress concentration and is somehow related to fracture mechanism. The purpose of this paper is to analyze various characteristics of this band pattern in light of physical mesomechanics, and discuss its relationship to fracture mechanism. It will be shown that the formation of this band pattern is essentially related to material fracture and that the related observations are well explained by the mesomechanical picture of fracture mechanism.

1. Introduction

Physical mesomechanics (PMM) is a recent theory of plastic deformation (PD) developed by Panin et. al [1]. To my best knowledge it is the only theory available to date that can formulate all the stages of PD including fracture on the same physical basis. Based on the principle of gauge invariance, PMM describes all the related dynamics on a complete physical basis, making its formalism universal and basically applicable to any heterogeneous medium. These features make PMM quite useful for various practical applications such as nondestructive evaluation of solid-state objects [2] and computer aided design of materials.

Mathematically, PMM describes PD as a $GL(3, R)$ transformation that the deformation structural element (DSE) undergoes under a given loading condition [3]. Here, the DSE is defined as a volume element in which a local reference frame can be setup. Different DSEs transform differently according to their own local frame. This is how the local gauge invariance is taken into consideration. Introducing a proper gauge field, PMM has derived a field equation that describes the relationship between the free field and the covariant current of the field of the local reference frame. This whole process is essentially analogous to the description of an electromagnetic field as a gauge field for $U(1)$ transformation. In fact, the field equation of PMM leads to a set of wave equations governing the translational and rotational modes of deformation, which are identical to the Maxwell equations of the electromagnetic theory. The resultant wave is called the plastic deformation wave (PDW).

Material scientifically, PMM interprets PD as a continuous process of stress relaxation. From this viewpoint, the PDW can be interpreted as a self-organized wave due to the synergetic interaction between translational and rotational modes of displacement through which the material relaxes stress energy. It should be noted that because of the spatial non-uniformity of the dynamics, this wave characteristic has a vortical nature that PMM calls the translational-rotational vortex (TRV). As the degree of PD progresses, the spatial non-uniformity enhances causing the scale level of the DSE to increase. This is accompanied by increases in the scale levels of the associated PDW and TRV. Based on this scale level, PMM classifies the stage of PD into the micro-, meso- and macro-level, where the meso-scale level plays an essentially important role in the development of PD to fracture.

An important consequence of the above-mentioned formalism is its capability of describing fracture as the final stage of PD. In PMM, the progress in PD is interpreted as phase transition that is accompanied by a change in the mechanism of stress relaxation. In an early stage of PD, the material relaxes stress energy through the propagation of PDW. As the degree of PD progresses, the defect density increases making the material dissipative, causing the PDW to decay as any wave decays when the system becomes dissipative. When the material becomes totally dissipative and therefore the PDW does not function as a mechanism of stress relaxation, discontinuity is generated in the material as the alternative mechanism of stress relaxation. This stage is interpreted as fracture. Importantly, fracture does not necessarily leads to failure. If fracture

takes place in a micro-level, the discontinuous situation is recoverable. However, if fracture takes place in the macro-level, it normally leads to failure of the material. Thus it is always important to observed PD taking its scale-level into consideration.

We are primarily interested in applying PMM to nondestructive evaluation (NDE). The uniqueness of such a NDE technique is its capability of predicting the location and timing of the failure of an object. Here the prediction is based on the above-mentioned decaying character that the PDW shows as the PD progresses. Specifically, in this decaying process the PDW shows the following features that PMM defines as the pre-fracture criteria [2]. (1) The wavelength of PDW becomes comparable to the sample size (wavelength criterion); (2) the PDW becomes stationary (stationary wave criterion); and (3) a pair of highly developed TRV having mutually opposite directions of rotation appear (vortex criterion).

Previously we have carried out a number of tensile experiments exploring for these pre-fracture criteria. Since the rate of displacement is the primary variable of the above-mentioned field equation after the summation over the group indexes, we consider that the displacement is the most important parameter to study the wave characteristics of PD, and analyzed displacement waves. We have employed an optical interferometric technique called electronic speckle pattern interferometry (ESPI) that allows us to measure displacement as a whole field, two-dimensional data. Consequently, we have observed the pre-fracture criteria in qualitative [2, 4] and semi-quantitative [5] ways.

In the course of these experiments, we discovered that the failure of a sample is always accompanied by the appearance of an interferometric band structure. Because this band structure appears conspicuously white on our black-and-white monitor we call it the white band (WB) [6]. From the viewpoint of NDE, the WB has the following important properties. If a WB is observed at various locations on the sample at different times, hence if it appears dynamic, the sample is still far from failure. If a WB is observed at a certain location of the sample, hence if it appears stationary, the sample can fail at any moment at that location. Thus by monitoring the movement of a WB, one can judge whether or not the sample is close to failure and where the failure will take place.

Since the discovery of the WB, we have investigated the formation of the WB under various conditions. Consequently, we have found that the formation of a WB is deeply related to stress concentration. If the sample is free of initial stress concentration, a WB normally begins to appear as soon as the sample enters the plastic region (past the yield point), and it appears dynamic until it becomes stationary at a certain location where the sample eventually fails. If the sample has initial stress concentration such as a weld, the WB tends to be less dynamic, and if the initial stress concentration is high it can be stationary from the beginning. Moreover, in the case that the initial stress concentration is very high, the WB can begin to appear in the elastic region (before the yield point), and it is stationary from the beginning. In any case, the sample always fails at the location where the WB becomes stationary. We have also found that the WB is formed along the boundary of a pair of TRV where a bend-torsion moment operates [4]. More recently, Q. Zhang et al. [7] have made more detailed analyses on the formation of WB and discovered that the formation of a WB actually has two stages where the first stage is characterized relatively slow deformation than the second stage.

These observations altogether indicate that the WB is an important parameter associated with the transition from the late stage of PD to the fracture stage. However, the information is somewhat fragmentary, and there has not been discussion on the formation of a WB in connection with the wave character of PD. Thus the purpose of this paper is to summarize the previously observed various properties of the WB more systematically as well as adding some new findings, and identify the WB in more clear, mesomechanical terms. Emphasis will be laid on describing the WB and its formation in reference to the mesomechanical interpretation of fracture and the basic wave equations that PMM has derived from the gauge theoretical consideration.

2. Speckle interferometry and tensile analysis

Fig. 1 illustrates a typical optical arrangement for ESPI [8]. When an object is illuminated by a coherent beam and imaged into a CCD (charge coupled device) camera, speckles are formed on its image plane as a consequence of interference among a number of rays randomly reflected on the object surface. While the phase relationship among the rays forming each speckle is at random, the speckle corresponds to a definite phase determined by the distance between the object and the light source as a result of coherent superposition of these rays. If the object is illuminated by a pair of coherent beams originating from the

same source, an interference speckle field is formed on the image plane. Here the word interference is used to mean the interferometric addition of the phases of speckles caused by the respective beams. Since these beams come from the same source, the resultant phase of the interference speckle is related to the optical paths of the respective beams. Therefore, if the object displaces rightward under this condition, as shown in Fig. 1 for example, the phase change of the interference speckles represents the decrease in the optical path of beam 1 and the increase in the optical path of beam 2. This phase change can be detected as changes in the speckle's intensities. Thus by monitoring such an intensity change at many points, the displacement can be extracted in the whole field.

More quantitatively, the intensity of an interference-speckle before (I_{bf}) and after (I_{af}) a displacement d can be expressed as shown below. Here q is the initial phase of the speckle, f is the phase change caused by the displacement, I_1 and I_2 are the averaged intensities of the respective beams, and f can be related to the displacement through the wavelength λ of the coherent light and the angle of incidence α . Thus by subtracting I_{af} from I_{bf} electronically, a fringe system representing $\sin(f)$ can be obtained. We call the image containing interference speckles specklegram, and the subtracted specklegram holding fringe system the subtracted interferogram.

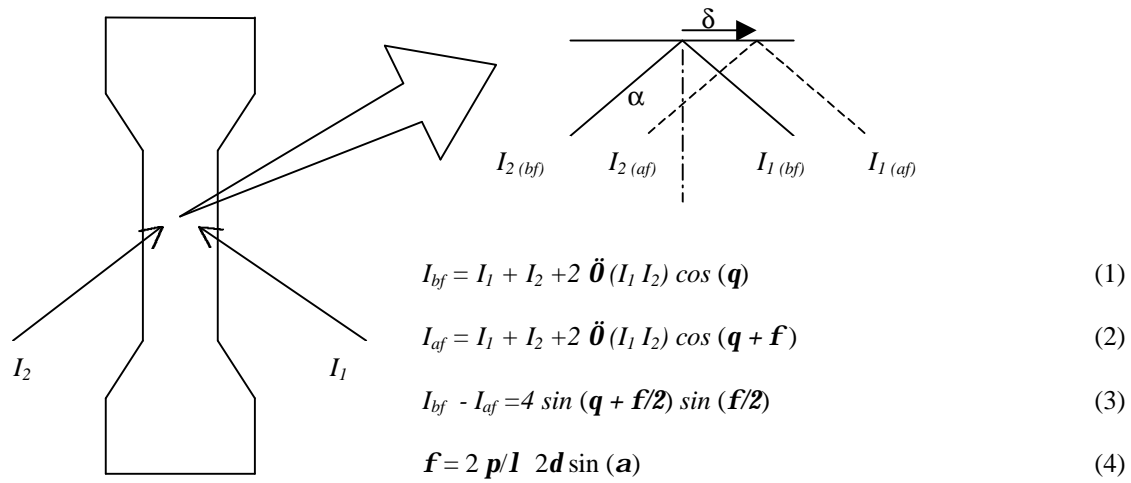


Fig. 1 Concept of ESPI. Suffixes bf and af denote before and after a displacement δ , respectively. α is the angle of incident.

In a tensile analysis, a CCD camera takes a specklegram at each time step with a constant interval, where the interval is chosen to be sufficiently small so that the resultant subtracted interferogram generates a proper number of fringes [2, 7]. The rate of displacement can be extracted from those interferograms by counting the orders of fringes [5]. Note that while these fringes are insensitive to the direction of the displacement, it is usually not too difficult to judge the direction by considering that the sample is elongated along the axis of the tensile load and contracts in the transverse direction. There are some techniques to determine the direction of displacement [9], which is useful for the cases in which the determination of the direction of the displacement is not straightforward.

A WB is formed in a fringe system formed on a subtracted interferogram. It is easily distinguished from the surrounding fringes because of its sharper edges and more uniform intensity. In one word, the formation of a WB can be understood by dense deformation concentrated in the region. Q. Zhang et al. [7] have observed how deformation is concentrated into the region of a WB by animated interferograms and found that the fringe density becomes too high to be resolved in the second stage of WB formation which is characterized by faster deformation [7]. In any case, the uniform intensity can be understood as the fringe density is higher than the spatial resolution, and the sharper edge is explained by the localization of the highly dense deformation. In terms of PMM terminology, this is the strain localization caused by concentrated deformation.

3. WB

Experimental arrangement to observe a WB and the general properties of WB are described in detail elsewhere [2, 6]. In short, a CCD camera takes specklegram containing the whole image of the sample under a tensile load and transfers its output to a frame grabber where image subtraction is performed to obtain a subtracted interferogram. When the degree of stress concentration reaches a certain level a WB is formed in the subtracted interferogram. In an early stage when the level of stress concentration is not critically high, WBs can be observed at various locations at different times, and therefore it appears that the WB is dynamic. When the stress concentration becomes so high that the deformation is concentrated at a certain point, a WB is repeatedly observed at that point until the sample fails there. These properties of the WB indicate that the formation of a WB is obviously caused by stress concentration and is somehow related to fracture mechanism. According to PMM, on the other hand, the fracture is a stage of PD in which the material becomes so dissipative that it cannot relax the stress energy by propagating a PDW. Under that condition, the synergetic interaction between the translational and rotational modes of deformation does not function. Consequently, the PD is characterized only by the rotational mode, and discontinuity is generated in the material as the alternative channel of stress relaxation [1]. Therefore, if the formation of a WB is associated with fracture, it should show these indications. In fact, there are some experimental observations that indicate that this is the case. These observations are: (1) The fringe pattern observed along with a WB represents bodily rotation of the sample indicating that the deformation is characterized by pure rotation [6, 7]. (2) The formation of a WB is accompanied by an abrupt stress relaxation that implies the generation of material discontinuity [2]. (3) A WB begins to appear when the PDW is about to completely decay indicating that the synergetic interaction between the translational and rotational modes of deformation stops functioning [5]. Below we will discuss these observations.

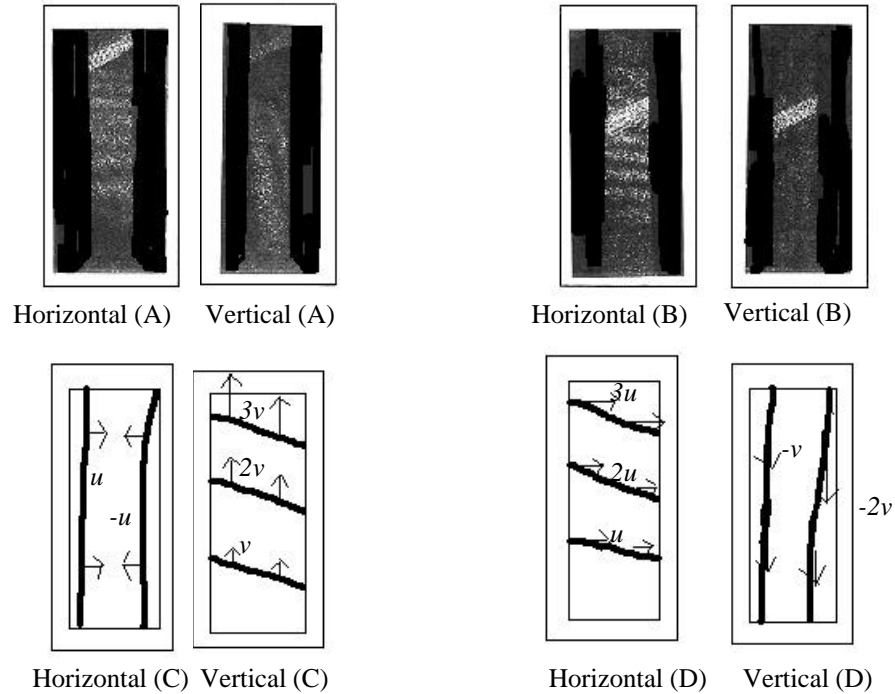


Fig. 2 (A), (B): Typical fringes observed together with a WB. (C) Fringe system representing relatively uniform vertical expansion and horizontal contraction. (D) Fringe system representing clockwise bodily rotation.

3.1 WB and rotational deformation

Fig. 2 shows typical fringe patterns observed in horizontally and vertically sensitive interferograms along with a WB. Here we use the words horizontally sensitive interferogram and vertically sensitive interferogram to mean subtracted interferograms generated by horizontally and vertically sensitive interferometers, respectively. (By this definition, the interferometer shown in Fig.1 is a horizontally sensitive interferometer.) Before discussing these particular fringe systems, let us consider general properties of fringe systems observed in horizontally and vertically sensitive interferograms. As easily understood from eq. (3) and the related explanation in Section 2, the dark fringes on a vertically sensitive interferograms represent the loci of vertical displacement v that corresponds to phase changes of a multiple of 2π . Therefore, if these fringes run horizontally in parallel to each other (Fig.2C), the whole interferogram represents relatively uniform elongation in which v increases as you go farther from the stationary grip. Indeed, this kind of fringe system is often observed when the sample is in the elastic region. If the fringes on a vertically sensitive interferograms run vertically in parallel to each other (Fig.2D), on the other hand, the interferogram represents a bodily rotation of the sample where v increases as you go farther from the center of the rotation. Similarly, vertically parallel fringes and horizontally parallel fringes on a horizontally sensitive interferogram represent, respectively, relatively uniform horizontal contraction and bodily rotation (Fig.2C and Fig. 2D).

Now if you observe the fringes on the respective sides of the WB in Fig. 2A and Fig. 2B, it is clear that the fringes in the horizontally sensitive interferogram are running horizontally and those in the vertically sensitive interferogram are running vertically. This indicates that the parts of the sample above and below the WB rotate rather bodily, presumably in mutually opposite directions indicating that the formation of a WB represents “the rotation only” situation that PMM defines as a criterion of fracture. In ref. [7]. the authors also state that toward the end of the formation of a WB, the sample show a rigid-body like motion. In addition, they claim that the formation of a WB can be divided into two stages; the first stage is characterized by relatively slow process in which the strain is localized into the region where the WB is formed, and the second stage is characterized by a faster process in which the density of fringes within the WB becomes too high to resolve. Fig. 7 of ref. [7] clearly shows that the above-mentioned fringe pattern representing a bodily rotation is observed in the second stage. These altogether strongly indicate that in the second stage of WB formation, the deformation is totally concentrated in the region of the WB and this causes the parts of the sample above and below the WB rotate rather bodily.

There is an independent experimental observation that indicates that these bodily rotations of the sample at the opposite side of a WB are in mutually opposite directions. Fig. 3 shows a two-dimensional vector field of $d\mathbf{V}(u, v)/dt$ observed one time step before a stationary WB begins to appear. It is seen that the region along which the WB appears one step later actually runs along the boundary of the two vortices. Since the physical unit of \mathbf{V} is velocity, $d\mathbf{V}/dt$ has a physical unit of acceleration and therefore is proportional to a force. This means that the mutually opposite vortices observed at the different sides of the

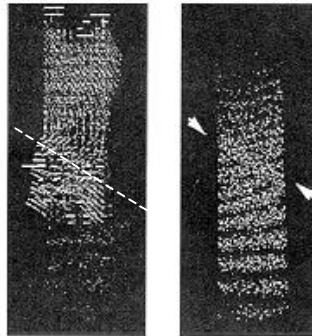


Fig.3 Vortexes of $\partial\mathbf{V}/\partial t$ field observed one time-step before a WB appears. Arrows indicate where the WB appears. Dashed line indicates boundary of vortexes.

WB represent the situation where a bent-torsion moment is operating in such a way that the sample is bent about the location of the WB. In addition, the fact that the dV/dt vectors along the WB on the different side on the sample are parallel means that there is no force operating across the WB region. This strongly indicates that discontinuity is generated in the WB region making this part of the sample stretched with no force (see next section).

3.2 WB and stress relaxation

Fig. 4 shows a time historical trace of the location of WBs and the corresponding loading curve. The sample used in this experiment is an aluminum alloy A5052H32. The sample size was 100 mm in effective length, 25 mm wide and 2 mm in thickness. The tensile speed was 0.35 mm/min. Apparently, this sample shows WBs of the dynamic type. It is seen that as soon as WBs begin to appear the loading curve starts to show a zigzag character [10] indicating that abrupt stress relaxation and work hardening take place alternatively. In a different sample that shows a WB of the stationary type we have observed that as soon as the WB begins to appear the stress drops abruptly and stayed at that level until the sample fails [2]. From this observation, it is thought that in the case of a dynamic WB the repetition of abrupt relaxation and work hardening takes place every time a WB appears at a different location. It is most likely that this abrupt relaxation corresponds to the large elongation that Q. Zhang et al. [7] have observed on the formation of a WB. Moreover, from the observations that the bodily rotation takes places in the second stage of WB formation and that the bodily rotation represents the rotation-only situation corresponding to the generation of discontinuity, it is likely that the abrupt stress relaxation occurs in the second stage of WB formation.

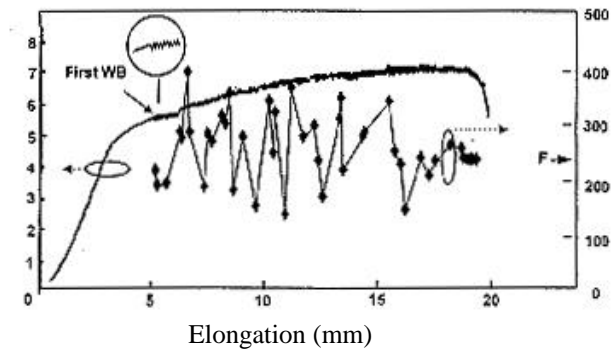


Fig.4 Appearance of WB and loading curve. Appearance of WBs is accompanied by zigzag stress fluctuation indicating sharp stress relaxation.

The above-mentioned relationship between abrupt relaxation and appearance of a WB indicates that when a WB is formed the state of the material changes drastically, implying that the appearance of a WB is somehow correlated to acoustic emission. Thus in the next experiment, we attached two acoustic emission sensors at the two ends of the sample and estimated the location of the source of emission at the same time as we took specklegrams to observe WBs. Here the location of acoustic emission was estimated from the difference in the time at which the respective sensors detected the signal.

Fig. 5 shows the locations of acoustic emission estimated in this way on the same time axis as the locations of the observed WBs. The sample used for this experiment was an aluminum alloy A6063, and the sample size was 100 mm in effective length, 25 mm in width and 1 mm in thickness. We gave a tensile load to this sample at a constant rate of 1 mm/min. As seen in Fig. 5, this sample showed WBs at three locations at three different times. These WBs run at some angle with respect to the tensile axis. The vertical error bars in Fig. 5 indicate the locations of each WB at the left and right side of the sample. The acoustic emission was detected in a finite time frame that was longer than the data acquisition time to generate one WB. The horizontal error bars represent this time frame. In this sample, we detected totally five acoustic emission signals in two time frames. Fig. 5 clearly shows that both of these time frames coincide with the

two of the three time frames in which WBs were observed. Moreover, the location of the acoustic emission was identical to that of the WBs in the first time frame, and at least the location of one acoustic signal detected in the second time frame was identical to the location of the WBs. These coincidences strongly indicate that an acoustic wave is emitted during the formation of a WB. It is most likely that an acoustic wave is emitted in the second stage of the WB formation, in which material discontinuity is presumably generated as discussed above.

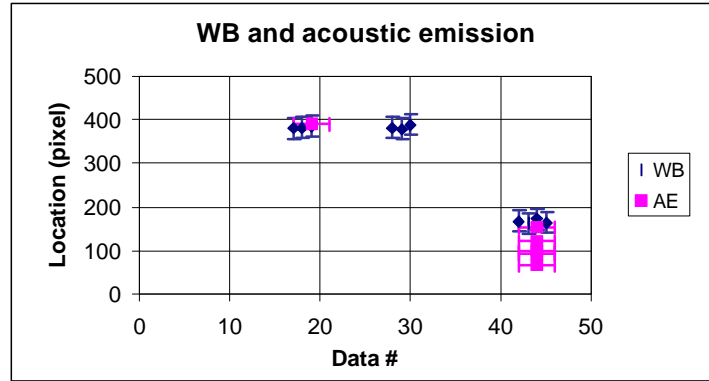


Fig.5 Appearance of WB and acoustic emission.

3.3 WB and PDW

Next we discuss the relationship between the PDW and WB using an experiment in which we actually extracted the rate of displacement at each time step by analyzing the fringes in the interferogram [5]. Fig. 6 shows an example of the result of such a measurement. The material used for this measurement is the same as Fig.5, whereas the tensile speed was 0.1 mm/min. In this measurement, we extracted displacement from horizontally sensitive interferograms along the tensile axis and plotted it as a function of time. Thus Fig.6 represents a PDW observed in the transverse component of the rate of displacement. In this figure, also presented is the time historical trace of the WB observed in the interferograms. Apparently, the WB observed in this sample is categorized as the stationary type. It is seen that the WB begins to appear when the PDW is about to lose its temporal variation, i.e., when it is about to decay. This supports the above consideration that the WB represents the “rotational-only” situation that the sample enters when discontinuity is generated leading to fracture. Indeed in Fig.6, the sample fails shortly after the WB appears and the PDW loses its temporal variation. Note that the final sharp rise of the PDW indicates the fact that the sample swings largely to a side when it fails.

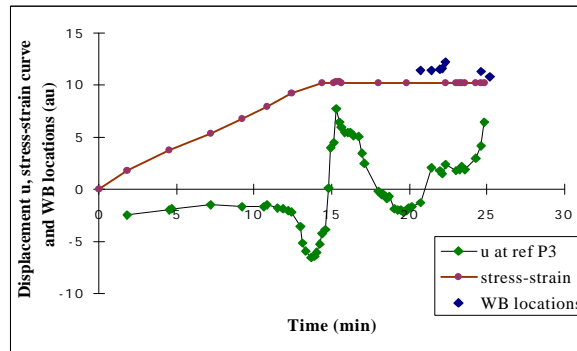


Fig.6 Decay of PDW and appearance of WB.

3.4 Mesomechanical interpretation of WB

From the above argument, it is clear that the WB appears at the boundary of macroscopic DSEs and represents the generation of material discontinuity. As mentioned above, according to PMM the material becomes discontinuous when the PDW decays. This implies that the WB should be somehow interpreted in connection with the wave characteristics of PD. In this section, an attempt is made to consider the formation of WB in light of the mesomechanical wave equations.

After summation over the group indexes, the field equation representing the synergetic interaction between the translational and rotational mode of PD can be expressed in the following form.

$$\text{div } \mathbf{V} = -g^{ij} \mathbf{h}_i \dot{\mathbf{h}}_j \quad (5)$$

$$\text{rot } \mathbf{V} = -\nabla \mathbf{w} / \nabla t \quad (6)$$

$$\text{rot } \mathbf{w} = (1/c_i^2) \nabla \mathbf{V} / \nabla t + g^{ij} \mathbf{h}_i D\mathbf{h}_j \quad (7)$$

$$\text{div } \mathbf{w} = 0 \quad (8)$$

where $\mathbf{V}(u, v)$ is the rate of displacement, c_i is the phase velocity, \mathbf{w} is the angle of rotation, g^{ij} is the metric tensor, \mathbf{h}_i is the local bench mark set up on the DSE of interest, and i and j are the internal indexes. The right-hand side of eq. (5),

$$-g^{ij} \mathbf{h}_i \dot{\mathbf{h}}_j = J_0$$

represents the source term associated with translational flow. The second term on the right-hand side of eq.(7),

$$g^{ij} \mathbf{h}_i D\mathbf{h}_j = \mathbf{J}$$

represents the current flowing along the boundary of DSEs associated with the rotation of the DSE as a whole. If you take div of eq.(7), it follows from the relationship $\text{div}(\text{rot } \mathbf{w})=0$ that

$$(1/c_i^2) \nabla J_0 / \nabla t + \text{div } \mathbf{J} = 0 \quad (9)$$

where eq.(5) is used in the first term on the left-hand side. Eq.(9) represents the current conservation rule.

When the material is in an early stage of PD where the propagation of a PDW is the channel of stress relaxation, the energy associated with the rotational motion of the previous phase is transferred to translational motion. Mathematically, this situation can be represented by the following wave equation.

$$\Delta \mathbf{V} - (1/c_i^2) \nabla^2 \mathbf{V} / \nabla t^2 = \nabla \mathbf{J} / \nabla t - \text{grad } J_0 \quad (10)$$

where the first term of the right hand side represents the rotation of the DSE as a whole and the second term represents the effect of the translational mode of displacement as an accommodation process for the rotational mode. When the translational-rotational interaction is effective as a relaxation channel, these two terms balance each other so that \mathbf{V} shows wave characteristics. When the PD progresses, the material becomes too dissipative to maintain a PDW, causing that the PDW decays and eventually loses its temporal variation completely, i.e. $\nabla \mathbf{V} / \nabla t = \mathbf{0}$. In this situation, from eq.(7), $\text{rot } \mathbf{w}$ tends to be sustained only by the DSE boundary current \mathbf{J} . Then from eq.(9),

$$\text{div } \mathbf{J} = 0. \quad (11)$$

Eq. (11) means that the current \mathbf{J} flows from one side of the DSE boundary to the other side without any net gain or loss (called the constant boundary current \mathbf{J}). If this takes place on a macroscopic level where

the DSE is comparable to the sample size, the current \mathbf{J} is expected to flow from one side of the sample to the other side.

As clear from Fig. 6 and the discussion made in Section 3.3, on the other hand, the WB is formed at the boundary of DSEs when $\|\mathbf{V}\|/t$ becomes small. In addition, a WB runs across the sample from one side to the other. Thus, it is most naturally interpreted that the WB represents a current \mathbf{J} that flows all the way along the boundary of macroscopic DSEs under the condition where $\|\mathbf{V}\|/t$ is small. Moreover, it is interpreted that the second stage of WB formation corresponds to the situation $\|\mathbf{V}\|/t = 0$, hence the condition $\text{div}\mathbf{J} = 0$ is satisfied. Note that this is the situation where with the lack of a new source J_0 being generated the total current is sustained only by the constant boundary current \mathbf{J} , and that this corresponds to the “rotation-only” situation where material discontinuity is generated being accompanied by acoustic emission.

It is interesting to note that under the condition of $\|\mathbf{V}\|/t = 0$, from eq. (9) the current \mathbf{J} is time independent. This means that on the right hand side of eq. (10) the first term is zero. Therefore unless the second term $\text{grad} J_0$ is zero, there is no possibility that the right hand side is zero, i.e. the wave character is preserved. However, under this situation, the strain is localized and $\text{grad} J_0$ is likely to be considerably large. This is the mathematical ground to explain why PDW decays.

4. Conclusions

The previously observed optical band structure was analyzed from the viewpoint of physical mesomechanics. It has been clarified that the formation of this optical band structure essentially represents the mesomechanical picture of fracture, which is characterized by rotational-only deformation, abrupt stress relaxation associated with the generation of material discontinuity, and decay of the plastic deformation wave. Mathematically, the WB corresponds to a constant boundary current that flows across the width of the sample. These observations justify the use of this optical band structure as an indicator of fracture in nondestructive evaluation. The author strongly feels that the application of physical mesomechanics to nondestructive testing and other engineering techniques is of great importance, and that for such applications the type of the optical interferometric method presented in this paper is useful. From this standpoint, he welcomes any comment or question from researchers and engineers of a wide variety of fields.

Acknowledgment

The author is grateful to Acad. V. E. Panin of Russian Material Center for precious discussion and advice. Discussion on the optical interferometry with Prof. S. Toyooka of Saitama University is also appreciated. Part of the experiment was made under collaboration with the Reactor Safety Technology Center (RSTC) of the Indonesian National Atomic Agency. The acoustic emission measurement was made with the assistance of M. H. Pardede, B. Siahaan, N. Sijabat, H. Simangunsong, T. Simbolon, and Histori and other staff members of RSTC. The author is very grateful for this assistance.

References

- [1] V. E. Panin, ed. Physical mesomechanics of heterogeneous media and computer-aided design of materials, Cambridge International Science, Cambridge (1998)
- [2] S. Yoshida, Muchiar, I. Muhamad, R. Widiastuti and A. Kusnowo, Opt. Exp. 2, (1998) 516
- [3] V. E. Egorushkin, Fiz. Izv. 33 (1990) 51
- [4] S. Yoshida, I. Muhamad, M. Pardede, R. Widiastuti, Muchiar, B. Siahaan and A. Kusnowo. Theor. Appl. Frac. Mech. 27 (1997) 85
- [5] S. Yoshida, B. Siahaan, M. H. Pardede, N. Sijabat, H. Simangunsong, T. Simbolon and A. Kusnowo, Phys. Lett. A, 251 (1999) 54
- [6] S. Yoshida, Suprapedi, R. Widiastuti, M. Pardede, S. Hutagalong, J. S. Marpaung, A. Faizal and A. Kusnowo, Jap. J. Appl. Phys. 35 (1996) L854
- [7] Q. Zhang, S. Toyooka, Z. Meng and Suprapedi, Proc. SPIE, 3585 (1999) 389

- [8] O. J. Lokberg, in: Speckle Methodology, ed. R. S. Sirohi, Optical Engineering, 38 (Marcel Dekker, New York, 1993) 163
- [9] For example, S. Yoshida, Suprapedi, R. Widiastuti, Marincan, Septriyanti, Julinda, A. Faizal and A. Kusnowo, Appl. Opt. 36 (1997) 266
- [10] V. E. Panin, in V. E. Panin, ed. Structural level of plastic deformation and fracture, Nauka, Novosibirsk (1990) 8